Proceedings of 14th IOE Graduate Conference
Peer Reviewed
Year: 2023 Month: December Volume: 14
ISSN: 2350-8914 (Online), 2350-8906 (Print)

Change in Irrigated Land Based on NDVI: A Case Study of Morang District

Pramit Ghimire [a], Saroj Karki [b], Vishnu Prasad Pandey [c] Ananta Man Singh Pradhan [d]

[a, c] *Department of Civil Engineering, Pulchowk Campus, IOE, Tribhuvan University, Nepal*
[b] *Ministry of Water Supply, Irrigation and Energy, Koshi Province, Government of Nepal*
[c] *Center for Water Resources Studies, Institute of Engineering, Tribhuvan University, Nepal*
[d] *Water Resources Research and Development Centre, Ministry of Energy, Water Resources and Irrigation, Government of Nepal*
[a] 078mswre007.pramit@pcampus.edu.np , [b] sarojioe@gmail.com, [c] vishnu.pandey@pcampus.edu.np, [d] anantageo@hotmail.com

Abstract

With the increasing demand for food and water resources due to population growth and climate change, accurate information about irrigated areas is crucial for effective planning and management. This study aims to quantify and analyze the variation of irrigated land in Morang district using remote sensing data for the last 10 years. The study utilizes Moderate Resolution Imaging Spectroradiometer (MODIS) Normalized Difference Vegetation Index (NDVI) images to calculate NDVI time-series and identify changes in irrigated and rainfed areas over time. Based on the NDVI time-series analysis three cropping cycle was seen in the study area with major crop during June to December. Using Random Forest Classifier, agricultural land was classified with an average overall accuracy of 0.88 and Kappa Coefficient of 0.77. Using MODIS NDVI data and agricultural land 250-m annual irrigated agricultural land was prepared for Morang district with the help of K-means clustering algorithm. In the last 10 years the irrigated land shows a fluctuating nature, however during the last three years has seen an increasing trend with 2022 being the year with most irrigated area: 1.08 lakhs hectare and 0.25 lakhs hectare rainfed land.

Keywords

Google Earth Engine, Irrigated Land, Machine Learning, MODIS NDVI, Remote Sensing

1. Introduction

With the irrigated areas accounting up to 40% of all land used for agricultural purposes, it is one of the largest consumers of water on a global scale [1]. According to the predictions,by 2050 Asia's water consumption would rise by 30–40% [2], with 80% of the demand going toward irrigation needs [3] . Hence, for those responsible for formulating policies and decisions, the spatial information is crucial to fulfilling the water demands. Agriculture, particularly on small traditional farms, plays a significant role in Nepal's economy. Most of such agriculture is carried out on small farms, typically less than 0.7 hectares , and is focused mainly on food production for local consumption. [4]. In addition, climate change is having an increasingly significant impact on agriculture in Nepal [5], with rising temperatures and more frequent extreme weather events like drought and severe floods affecting crop yields [6].

The application of remote sensing technology has created new avenues for monitoring and tracking the irrigated land [7], and it has proven successful in pinpointing the positions and dimensions of these regions, increasing the precision of data within particular political borders [8, 9]. Based on the reflectance from the canopy, various Vegetation Indices (VIs) have been introduced for quantification of irrigated land over the years. Normalized Difference Vegetation Index (NVDI) is one of the most commonly used VI [10]. NDVI is defined as [11]:

$$NVDI = \frac{NIR - R}{NIR + R} \tag{1}$$

where,

NIR = Near-infrared Radiation
R = Red Radiation

NDVI values fall within the range of -1.0 to 1.0, with elevated values indicating the presence of lush green vegetation and lower values signifying the prevalence of various non-vegetative surface . NDVI values near 0 generally correspond to bare soil, while negative NDVI values are typically associated with water bodies [?]. Traditional processing methods find it difficult to handle the progressively larger amounts of remotely sensed data and products [7] . The once slow and laborious pre-processing, processing, and post-processing techniques are being replaced by the use of machine learning algorithms integrated into cloud-based computing platforms like Google Earth Engine (GEE) [12]. To deal with the large amount of data, use of GEE is very helpful [13]. With rising temperature projections in the future, the need for irrigation may increase which could result in higher demands for irrigation water [14]. Water resources planning and management in agriculture need spatially-explicit information on the irrigated area. So, reliable data regarding the irrigated land is crucial for the effective planning and management.Various studies have been done on a global scale for the identification of irrigated areas with comparatively low-resolution data, some of which include FAO database [9] the GMIA 5.0 [15], and the MIRCA2000 [16]. This study aims to quantify the variation of irrigated and rainfed areas in Morang district over the last 10 years with a resolution of 250 m.

2. Study Area and Data

2.1 Study area

The study area for this research is Morang district as shown in Figure 1. The majority of study area falls in the Terai region and remaining on the Siwalik and Middle Mountain. The Terai region has the highest crop productivity due to its favorable geographical location, fertile land, and good climate conditions. The soil of the district is divided into three categories based on land, elevation and soil texture as Sandy loam (hill range); Loam and Clay (Chure range), and Sandy Clay Loam and Loam (Terai range). Rice is the main crop grown in the Terai region alongside wheat and maize. The yield of major cereal crops (Paddy, Maize, Wheat, Millet, Barley and Buckwheat) in 77/78 fiscal year is 4.03 ton according to Ministry of Agriculture and Livestock Development (MoALD).

The total area of Morang district is 1,855 km^2. Morang is one of the most populous districts in Nepal, with a population of over 1 million people[17].

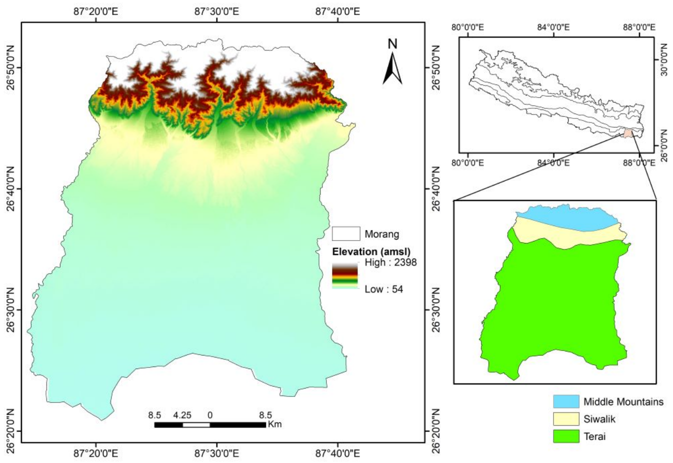

Figure 1: Location and details of study area

2.2 Data description

Landsat 8 images were used for the land use land cover classification. Landsat Collection 2 data represent a significant improvement in data processing, algorithm development, data accessibility, and enhanced distribution capabilities compared to Collection 1. Tier 1 Top of Atmosphere (TOA) was preferred to Tier 2 due to its better radiometric qualities [18]. Similarly, MOD13Q1.061 Terra Vegetation Indices with 250 m spatial resolution and 16-day temporal resolution was used. Savitzky-Golay filter was used to smooth out the noise in NDVI time-series, specifically that caused primarily by cloud contamination and atmospheric variability [19]. The reference data for land use classification was prepared using agricultural land data from Department of Water Resources and Irrigation (DoWRI). The Table 1 shows the summary of data used during this study.

Table 1: Data Sources

Data	Source	Spatio-temporal Resolution	Remarks
MOD13Q1.061 Terra Vegetation Indices	USGS	250 m, 16-Day Global; 2000-Now	To develop NDVI map, irrigated and rainfed map
Irrigation Map of Nepal	DoWRI	2015	To classify land use land cover
Landsat 8 Collection 2 Tier 1 TOA Reflectance	USGS	30-m, 16-Day Global; 2013-now	For agricultural land classification

3. Methodology

The overall framework of methods used is as shown in Figure 2

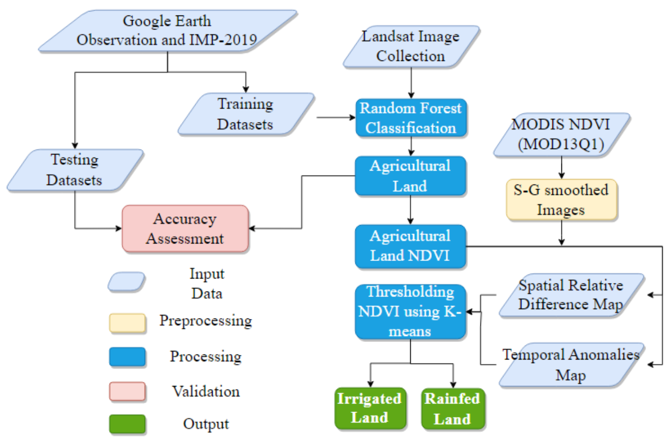

Figure 2: Methodological Framework

3.1 Pre-processing of images

Landsat images containing cloud cover and cloud shadow were masked using bitwise operator. The information contained in QA band was stored as Bitwise Flags. Then the pixel containing QA band value 3(Cloud) and 4(Cloud Shadow) were masked to get cloud free images. Based on the assumptions that NDVI time-series follow annual cycles of growth and decline of vegetation, and that clouds or poor atmospheric conditions usually depress NDVI values, Savitzky-Golay filter was used to smooth out the noise in NDVI time-series, specifically that caused by cloud contamination and atmospheric variability [19].

3.2 Land use land cover classification

The random forest was chosen primarily for its versatility and its ability to generate reasonably accurate land use classifications even without the need for extensive hyper-parameter tuning. It is suitable for a wide range of tasks, including both classification and regression [20]. For classification independent classification, which involved training a model on a single year with reference data from that year and same model was applied on different images without any changes or additional samples was used. [21].

The Random Forest classifier for the year 2015 was set-up using the reference data from Irrigation Master Plan-2019. The classifier contained two field: agricultural land and others (which include built-up area, forest cover, waterbody, etc.,). The reference data were split into training and testing samples in the ratio of 70:30. The model was trained using the training samples and validation was done via testing samples. Afterwards, the independent classification technique was used i.e., using the RF classifier for the year 2015, images of 2013 and 2022 were classified.

3.3 Definition of irrigated areas

The irrigated area is defined as the agricultural area that receives enough water for its growth and rainfed land imples the agricultural land which has not received adequate water. The mapping unit is maintained as 6.25 hectares, which corresponds to the MODIS 250-m pixel spatial resolution.

3.4 Distinction between irrigated and rainfed areas

Using the median reducer, the Savitzky-Golay filtered image collection was reduced over the study area to obtain a median value of each image and the time-series of median values were plotted to observe the NDVI cycle. This time series demostrated the median cropping cycle over the study area.

Concept of temporal stability can be very useful in deriving different indices that help to distinguish irrigated and rainfed lands [8]. A temporal-mean NDVI image during a cycle for Temporal anomalies index was also generated and finally a spatial-mean NDVI image during the peak NDVI was generated for determining relative spatial differences index [8]. These indices were calculated for each region separately, due to difference in cropping cycle in the regions.

$$\text{Spatial Relative Difference(SRD)} = \frac{\theta_{x,t} - \bar{\bar{\theta}}_t}{\bar{\bar{\theta}}_t} \tag{2}$$

$$\text{Temporal Anomalies (TA)} = \frac{\theta_{x,t} - \bar{\bar{\theta}}_x}{\bar{\bar{\theta}}_x} \tag{3}$$

SRD measures the extent to which the NDVI at a specific location on a given day deviates from the average NDVI across all locations for that same day. TA measures how much the NDVI value in a certain observation day differs from the temporal mean. K-means algorithm was utilized to generate high-resolution binary maps that distinguished between irrigated and non-irrigated areas based on these two features: SRD and TA.

4. Results and Discussion

4.1 Land Use Land Cover(LULC) changes and NDVI time-series

The classifier was built using the reference data in the year 2015, from irrigation master plan, which was then used to other composite images to classify the agricultural land for different years. The overall accuracy of the classifier was 0.88 and Kappa Coefficient was 0.77.

NDVI time-series was prepared for the agricultural area of Morang using mean reducer. The Figure 3, shows the mean NDVI time-series of Morang district from 2013 to 2022. The major cropping period is from June to December (Ashar-Mangsir). This period was used to calculate the indices for classification.

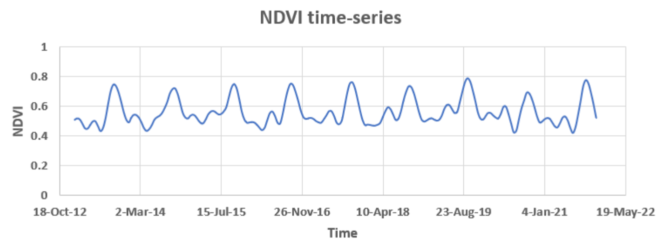

Figure 3: NDVI time-series

The average NDVI distribution over the district for the year 2013 and 2022 is shown in Figure 4. It shows increase in NDVI distribution especially in the middle mountain region.

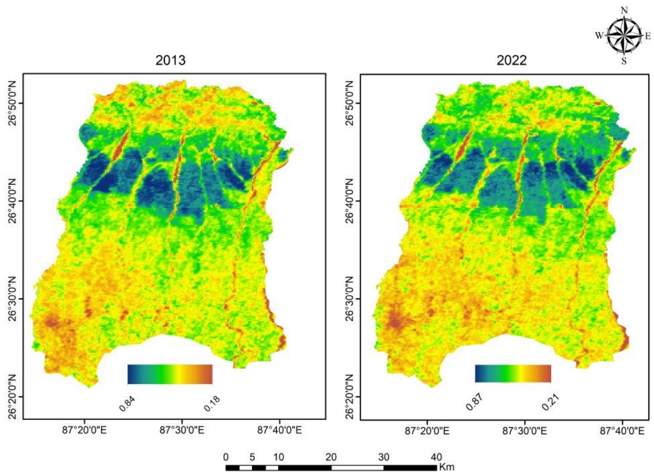

Figure 4: NDVI distribution: 2013(left) and 2022(right)

4.2 Classification of irrigated and rainfed land

K-means clustering algorithm was used to classify the agricultural areas to irrigated and rainfed land based on the indices. The Figure 5 shows irrigated maps for the year 2013 and 2022. Figure 6 shows the variation of irrigated and rainfed land through out the years. A significant increase in irrigated area has been observed in the last three years. The increase in irrigated areas has shown a 25.7% increase in production of cereal crops in Morang district according to statistical data from Ministry of Agriculture and Livestock Development from 2015 to 2022.

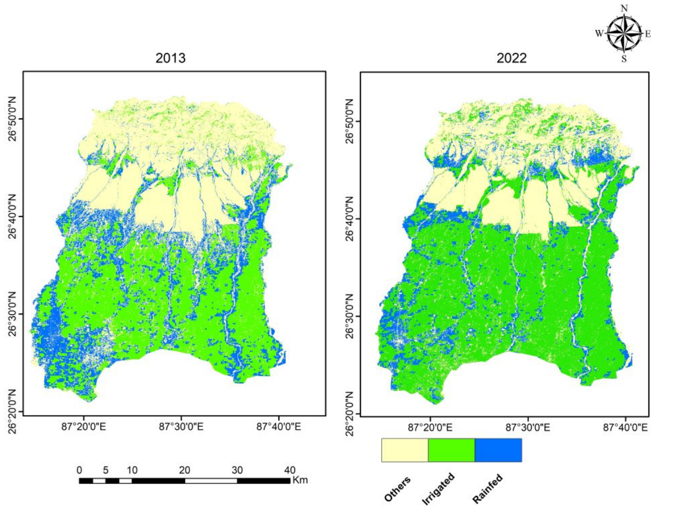

Figure 5: Irrigation map for the year 2013(left) and 2022(right)

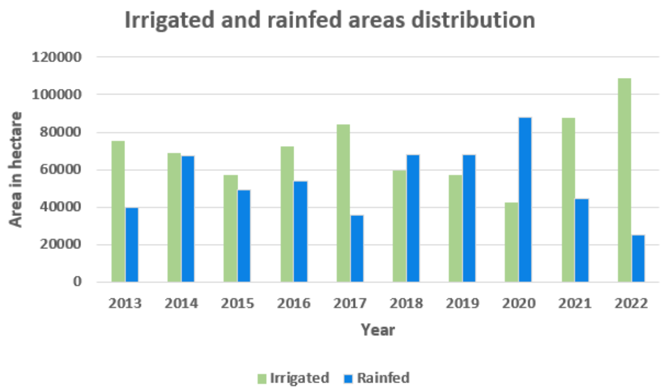

Figure 6: Irrigated and Rainfed areas distribution in Morang district

4.3 Uncertainties and limitations

Several factors may have led to some limitation on the result. Some of them are listed here.

- The satellite image used in this study, MODIS NDVI image collection, has a spatial resolution of only 250m (6.25 hectares area per pixel), so this may not capture the fine-scale variations in irrigated land, especially in regions with small irrigation systems.
- The pixel quality could also be another reason for potential misclassification of irrigated and rainfed land. Though a filter is used in the study to reduce the cloudy pixel effect, but actual value of the NDVI may not observed which may have limited the result.
- A temporal resolution of 16 days may not have been able to capture the maximum value of NDVI.
- Ground truth validation of each year will not be possible to validate the results.
- The error in the initial classification of agricultural areas may have contributed to errors in thresholding the stability indices.
- Resolution of MODIS NDVI could also be a potential source for overestimation of irrigated area.

5. Conclusions

The study explores the application of concept of temporal stability, for distinction of irrigated and rainfed areas. This method was applied to Morang district of the eastern Nepal. The irrigated and rainfed areas were classified based on the vegetation index NDVI in the GEE platform.

The NDVI time series shows two major cropping cycle in Terai, with June to December (Ashar- Mangsir) taken to the threshold between irrigated and rainfed land. After the distinction between irrigated and rainfed land, a significant increase in irrigated area has been seen in the last three years. On a decadal perspective, there was increase in irrigated land by 44.5%.

The results have several implications. For example, the increase in irrigated land have led to higher crop yields and more consistent production, with 25.7% increase in production of cereal crops in Morang district as per the statistical data from the Ministry of Agriculture and Livestock Development. The move towards increase in irrigated areas has the potential to trigger socioeconomic transformations in rural areas, leading to adjustments in long-standing agricultural methods, affecting people's ways of making a living, and potentially shaping the movement of people as employment prospects in agriculture undergo shifts.

Acknowledgments

The authors are thankful to Water Resources Research and Development Center (WRRDC) for supporting the research through “Project/Thesis Interns and Researcher Mobilization Program (SN: 11.5.40.89)”

References

[1] FAO. Did you know . . . ? facts and figures about, http://www.fao.org/nr/water/aquastat/didyouknow/index3.stm (last access: 9 september 2023). 2014.

[2] Alberto Boretti and Lorenzo Rosa. Reassessing the projections of the world water development report. *NPJ Clean Water*, 2(1):15, 2019.

[3] Yusuke Satoh, Taher Kahil, Edward Byers, Peter Burek, Günther Fischer, Sylvia Tramberend, Peter Greve, Martina Flörke, Stephanie Eisner, Naota Hanasaki, et al. Multi-model and multi-scenario assessments of asian water futures: The water futures and solutions (wfas) initiative. *Earth's Future*, 5(7):823–852, 2017.

[4] CIAT World Bank, CCAFS, and LI-BIRD. Climate-smart agriculture in nepal. csa country profiles for asia series, 2017.

[5] Douglas James Merrey, Abid Hussain, Deepak Dorje Tamang, Bhuwan Thapa, and Anjal Prakash. Evolving high altitude livelihoods and climate change: a study from rasuwa district, nepal. *Food Security*, 10:1055–1071, 2018.

[6] D Bocchiola, L Brunetti, A Soncini, F Polinelli, and M Gianinetto. Impact of climate change on agricultural

productivity and food security in the himalayas: A case study in nepal. *Agricultural systems*, 171:113–125, 2019.

[7] Liping Yang, Joshua Driscol, Sarigai Sarigai, Qiusheng Wu, Haifei Chen, and Christopher D Lippitt. Google earth engine and artificial intelligence (ai): a comprehensive review. *Remote Sensing*, 14(14):3253, 2022.

[8] Jacopo Dari, Luca Brocca, Pere Quintana-Seguí, Stefano Casadei, María José Escorihuela, Vivien Stefan, and Renato Morbidelli. Double-scale analysis on the detectability of irrigation signals from remote sensing soil moisture over an area with complex topography in central italy. *Advances in Water Resources*, 161:104130, 2022.

[9] Mutlu Ozdogan, Yang Yang, George Allez, and Chelsea Cervantes. Remote sensing of irrigated agriculture: Opportunities and challenges. *Remote sensing*, 2(9):2274–2304, 2010.

[10] Anukesh Krishnankutty Ambika, Brian Wardlow, and Vimal Mishra. Remotely sensed high resolution irrigated area mapping in india for 2000 to 2015. *Scientific data*, 3(1):1–14, 2016.

[11] FJ Kriegler. Preprocessing transformations and their effects on multspectral recognition. In *Proceedings of the Sixth International Symposium on Remote Sesning of Environment*, pages 97–131, 1969.

[12] Pardhasaradhi Teluguntla, Prasad S Thenkabail, Adam Oliphant, Jun Xiong, Murali Krishna Gumma, Russell G Congalton, Kamini Yadav, and Alfredo Huete. A 30-m landsat-derived cropland extent product of australia and china using random forest machine learning algorithm on google earth engine cloud computing platform. *ISPRS journal of photogrammetry and remote sensing*, 144:325–340, 2018.

[13] Haifa Tamiminia, Bahram Salehi, Masoud Mahdianpari, Lindi Quackenbush, Sarina Adeli, and Brian Brisco. Google earth engine for geo-big data applications: A meta-analysis and systematic review. *ISPRS Journal of Photogrammetry and Remote Sensing*, 164:152–170, 2020.

[14] Xiao-jun Wang, Jian-yun Zhang, Shamsuddin Shahid, Enhong Guan, Yong-xiang Wu, Juan Gao, and Rui-min He. Adaptation to climate change impacts on water demand. *Mitigation and Adaptation Strategies for Global Change*, 21:81–99, 2016.

[15] Stefan Siebert, Petra Döll, Jippe Hoogeveen, J-M Faures, Karen Frenken, and Sebastian Feick. Development and validation of the global map of irrigation areas. *Hydrology and Earth System Sciences*, 9(5):535–547, 2005.

[16] Felix T Portmann, Stefan Siebert, and Petra Döll. Mirca2000—global monthly irrigated and rainfed crop areas around the year 2000: A new high-resolution data set for agricultural and hydrological modeling. *Global biogeochemical cycles*, 24(1), 2010.

[17] National Statistics Office. National population and housing census. 2021.

[18] USGS. Landsat collections.http://pubs.er.usgs.gov/publication/fs20183049. 812, 2018.

[19] Jin Chen, Per Jönsson, Masayuki Tamura, Zhihui Gu, Bunkei Matsushita, and Lars Eklundh. A simple method for reconstructing a high-quality ndvi time-series data set based on the savitzky–golay filter. *Remote sensing of Environment*, 91(3-4):332–344, 2004.

[20] Mohammadreza Sheykhmousa, Masoud Mahdianpari, Hamid Ghanbari, Fariba Mohammadimanesh, Pedram Ghamisi, and Saeid Homayouni. Support vector machine versus random forest for remote sensing image classification: A meta-analysis and systematic review. *IEEE Journal of Selected Topics in Applied Earth Observations and Remote Sensing*, 13:6308–6325, 2020.

[21] Cristina Gómez, Joanne C White, and Michael A Wulder. Optical remotely sensed time series data for land cover classification: A review. *ISPRS Journal of photogrammetry and Remote Sensing*, 116:55–72, 2016.